THE JOURNAL OF PHYSICAL CHEMISTRY B

Article

pubs.acs.org/JPCB

Carotenoid Charge Transfer States and Their Role in Energy Transfer Processes in LH1−RC Complexes from Aerobic Anoxygenic Phototrophs

Václav Šlouf,[†] Marcel Fuciman,[†,‡] Alexander Dulebo,[†] David Kaftan,[†] Michal Koblížek,[†,§] Harry A. Frank,[‡] and Tomáš Polívka*[,†,∥]

[†]Faculty of Science, University of South Bohemia, Branišovská 31, 370 05 České Budějovice, Czech Republic

[‡]Department of Chemistry, University of Connecticut, 55 North Eagleville Road, Storrs, Connecticut 06269-3060, United States

[§]Institute of Microbiology, Department of Phototrophic Microorganisms − Algatech, 379 81 Třeboň, Czech Republic

[∥]Biological Centre, Czech Academy of Sciences, Branišovská 31, 370 05 České Budějovice, Czech Republic

Supporting Information

ABSTRACT: Light-harvesting complexes ensure necessary flow of excitation energy into photosynthetic reaction centers. In the present work, transient absorption measurements were performed on LH1−RC complexes isolated from two aerobic anoxygenic phototrophs (AAPs), *Roseobacter* sp. COL2P containing the carotenoid spheroidenone, and *Erythrobacter* sp. NAP1 which contains the carotenoids zeaxanthin and bacteriorubixanthinal. We show that the spectroscopic data from the LH1−RC complex of *Roseobacter* sp. COL2P are very similar to those previously reported for *Rhodobacter sphaeroides*, including the transient absorption spectrum originating from the intramolecular charge-transfer (ICT) state of spheroidenone. Although the ICT state is also populated in LH1−RC complexes of *Erythrobacter* sp. NAP1, its appearance is probably related to the polarity of the bacteriorubixanthinal environment rather than to the specific configuration of the carotenoid, which we hypothesize is responsible for populating the ICT state of spheroidenone in LH1−RC of *Roseobacter* sp. COL2P. The population of the ICT state enables efficient S_1/ICT-to-bacteriochlorophyll (BChl) energy transfer which would otherwise be largely inhibited for spheroidenone and bacteriorubixanthinal due to their low energy S_1 states. In addition, the triplet states of these carotenoids appear well-tuned for efficient quenching of singlet oxygen or BChl-a triplets, which is of vital importance for oxygen-dependent organisms such as AAPs.

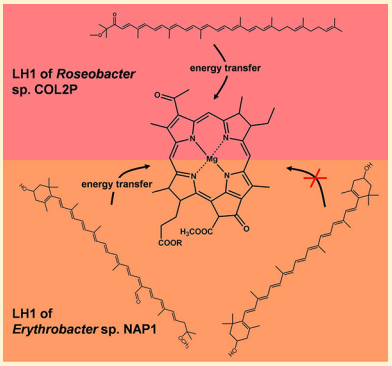

INTRODUCTION

Light harvesting is the first step in the transformation of light energy in photosynthesis. In this process, light is collected by pigment−protein complexes and subsequently delivered to the reaction center where it triggers redox processes.[1] In contrast to the largely conserved architecture of the photosynthetic reaction centers, light-harvesting complexes from different photosynthetic organisms exhibit a large variation in both structure and pigment composition.[2] Many investigations into the mechanism of light harvesting have focused on the relatively few antenna systems whose structures have been determined to atomic resolution: the Fenna−Matthews−Olson (FMO) complex of green sulfur bacteria,[3−6] the LH2 protein of purple nonsulfur bacteria,[7−11] the LHCII complex of algae and plants,[12−16] and the peridinin−chlorophyll *a*−protein (PCP) of dinoflagellates.[17−21] These studies revealed how the spectroscopic properties and precise arrangement of the two major classes of light-harvesting pigments, (bacterio)-chlorophylls ((B)Chls) and carotenoids, affect the efficiency and pathways of energy flow within antenna systems.

Light-harvesting systems from various photosynthetic microorganisms exhibit large variability in energy transfer efficiencies and pathways. In many cases, this can be attributed to the different positions of the excited states of the various carotenoids bound in the complexes. It is now well-established that carotenoids have two excited states which act as energy donors to (B)Chl: the S_2 state which is responsible for the strong absorption in the blue-green region and the dark S_1 state, which is located below the S_2 state and is forbidden for one-photon transitions from the ground state.[22] Whether S_2, S_1, or both states act as energy donors depends in large part on the conjugation length (N, number of the conjugated C=C bonds) of the carotenoid.[23] A few other dark states have been suggested to reside in the vicinity of S_1 and S_2,[24,25] but their involvement in energy transfer is still a matter of controversy.[26] The large complexity of the carotenoid excited-state manifold

Special Issue: Rienk van Grondelle Festschrift

Received: September 18, 2012
Revised: November 1, 2012
Published: November 6, 2012

and the underlying dynamics was recently also confirmed by theoretical studies.[27,28] Moreover, certain functional group substitutions, especially conjugated carbonyl groups, may significantly alter the spectroscopic properties and position of the energy levels of carotenoids,[29,30] and this has important consequences for the rate and efficiency of energy transfer.[20]

The crucial role of carotenoids in tuning light-harvesting properties of photosynthetic organisms has been demonstrated in a number of antenna systems. For example, although it is known that the LH2 complex shares many structural similarities with LH1,[31] it was recently reported that the population of the intramolecular charge transfer (ICT) state of a carbonyl carotenoid occurs only in LH1.[32] Also, LH1-specific carotenoid−protein interactions facilitate ultrafast carotenoid triplet state formation that is not observed in LH2.[32,33] Large variability of energy transfer pathways and efficiencies, which depends on carotenoid composition, has been also reported in many light-harvesting proteins with unknown high-resolution structure.[34−38]

Aerobic anoxygenic phototrophs (AAPs) represent a group of prokaryotes that contain reaction centers having BChl as the primary pigment. In contrast to their closest relatives, the purple nonsulfur bacteria, AAPs are obligatory aerobes that utilize organic matter as a main source of energy. Light serves only as an auxiliary energy source. AAPs do not form a compact phylogenetic group. Instead, they are dispersed among various subclasses of α-, β-, and γ-proteobacteria.[39,40] They account for an appreciable fraction of the microbial biomass in the upper ocean,[41,42] where they contribute significantly to the secondary (bacterial) production and recycling of organic matter.[43] Spectroscopic characterization of AAP light-harvesting systems revealed that they resemble those of purple nonsulfur bacteria including active energy transfer between carotenoids and BChl-*a*.[44,45] However, AAPs live in the presence of oxygen, and they synthesize predominantly oxygenated carotenoids (xanthophylls). These pigments may contain a conjugated carbonyl group known to influence the energy transfer mechanism in some photosynthetic organisms through the involvement of an ICT state.[20,32,34,35]

It is well-known that incorporation of carbonyl-carotenoids into some light-harvesting complexes facilitates S_1-mediated energy transfer[20,34,35] through strong coupling of the ICT state to the S_1 state.[30,46−49] The "activation" of the ICT state and its coupling to the S_1 state is readily observed in transient absorption spectra, as evidenced by specific spectral bands in the visible region associated with the ICT state. Typically, an ICT transition appears as a separate spectral band that is red-shifted compared to the strong S_1-S_N transition of carotenoids.[29,30] A coupled S_1/ICT state is likely to enhance energy transfer over what would be expected based on the S_1 route alone because of larger coupling of the S_1/ICT state to the acceptor state.[20] This light-harvesting strategy is apparently common among certain genera of marine algae and diatoms that utilize carbonyl carotenoids,[18,34,35] but very recently we have also found significant involvement of the ICT state in energy transfer in the spheroidenone-containing LH1 complex from *Rhodobacter* (*Rba.*) *sphaeroides*.[32]

Only recently have details concerning energy transfer pathways been revealed by femtosecond time-resolved spectroscopy applied to the LH4 antenna complex from the AAP *Roseobacter denitrificans*.[50] This particular LH4 complex contains the carbonyl carotenoid spheroidenone that transfers energy to BChl-*a* from both S_1 and S_2 states, though the overall energy transfer efficiency is lower than reported for the spheroidene-containing LH2 from the purple nonsulfur bacterium *Rba. sphaeroides*.[50,51] However, as reported for the LH2 complex from *Rba. sphaeroides*, no population of the ICT state of spheroidenone was observed in the LH4 complex from *Roseobacter denitrificans*, although a weak band attributable to the ICT state is present in transient absorption spectra of LH4 at 10 K.[50]

To examine whether the ICT state is also populated in light-harvesting complexes from AAPs, we examined LH1−RC complexes isolated from two species, *Roseobacter* sp. COL2P[45] and *Erythrobacter* sp. NAP1.[44] The LH1−RC complex from *Roseobacter* sp. COL2P binds the sole carotenoid, spheroidenone (Figure 1).[45] In contrast to *Roseobacter denitrificans*, it

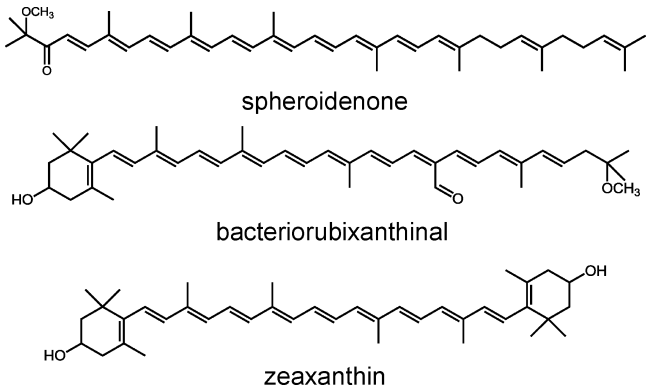

Figure 1. Structures of carotenoids in LH1−RC complexes of *Roseobacter* sp. COL2P (spheroidenone) and *Erythrobacter* sp. NAP1 (bacteriorubixanthinal and zeaxanthin).

contains only an LH1−RC core complex. In view of the recent report that spheroidenone exhibits markedly different behavior in LH1 and LH2 complexes of *Rba. sphaeroides*,[32] it is interesting to ask whether this property exists in light-harvesting complexes of AAPs. The LH1−RC complex from *Erythrobacter* sp. NAP1 contains the oxygenated carotenoids zeaxanthin and bacteriorubixanthinal (Figure 1).[44] Whereas zeaxanthin is a common xanthophyll found in cyanobacteria, algae, and plants and does not contain a conjugated carbonyl group, bacteriorubixanthinal has a carbonyl attached asymmetrically as an aldehyde functional group on the polyene chain (Figure 1). A similar arrangement of the conjugated carbonyl occurs also in peridinin where the effects of the ICT state are the strongest among naturally occurring carotenoids.[29,30] Thus, the application of femtosecond transient absorption spectroscopy to LH1−RC complexes isolated from these two species of AAPs provides an ideal opportunity to examine the effects of the conjugated carbonyl group on the rates and efficiencies of carotenoid to bacteriochlorophyll energy transfer in LH1-type light-harvesting complexes.

MATERIALS AND METHODS

Sample Preparation. *Erythrobacter* sp. NAP1[44] and *Roseobacter* sp. COL2P[45] cells were grown in a synthetic seawater medium containing 3 mM glutamate as described earlier.[45] Cells were harvested by centrifugation (15 000*g*, 15 min, 4 °C) and washed twice with a 50 mM Tris-HCl, pH = 8 buffer containing 1 mM EDTA and 50 mM NaCl. Washed cells were diluted with the same buffer (1:5 ratio) containing 1 mM phenylmethanesulfonylfluoride (PMSF) and broken by passage

dx.doi.org/10.1021/jp309278y | J. Phys. Chem. B 2013, 117, 10987−10999

through a French pressure cell at 20 000 psi. Cellular membranes were collected by ultracentrifugation at 100 000*g* for 2 h at 4 °C. The collected membranes were resuspended in buffer A (50 mM Tris-HCl, pH = 7.5, 10 mM $MgCl_2$, 10 mM $CaCl_2$, 50 mM NaCl, 1 mM EDTA), containing 20% glycerol and homogenized. Then, a solution of lauryldimethylamine-oxide (LDAO, 1% final concentration) was added, and the membranes were solubilized by stirring for 2 h (4 °C) in the dark. Insolubilized material was removed by ultracentrifugation (100 000*g*, 2 h, 4 °C). The supernatant containing photosynthetic complexes was further purified by ion-exchange chromatography on a DEAE-sepharose column (GE healthcare) equilibrated with buffer A containing 0.05% lauryldimethylamine-oxide (LDAO) ("eluent"). The crude LH1−RC was loaded on the column and equilibrated with the eluent, and then the NaCl concentration was linearly increased to 0.5 M. Purified LH1−RC fractions were eluted from the column at ∼0.3 M NaCl. The collected LH1−RC-containing fraction (A870/A280 > 1) was concentrated using a centrifugal filter (100 000 MWCO, Millipore), washed with buffer A, and concentrated again by ultracentrifugation to OD_{870} = 9 cm^{-1}. The purified LH1−RC was then subjected to a sucrose density gradient (100 000*g*, 20 h, 4 °C) prepared using buffer A containing 0.5 M sucrose, frozen, and thawed to produce a continuous gradient. The main LH1−RC band was collected and then again subjected to the centrifugal washing and concentration procedure described above. The LH1−RC preparation thus obtained had an A870/A280 ratio of >1.45 and was stored at −80 °C until used in the spectroscopic measurements.

Bacteriorubixanthinal was isolated by a preparative reverse-phase HPLC. The separation was conducted using a preparative Luna 3μ C8 column (Phenomenex, USA) and ammonium acetate-methanol:methanol solvent system as described earlier.[45] The HPLC fraction containing bacteriorubixanthinal was collected and transferred by two-phase extraction into chloroform. The chloroform phase containing bacteriorubixanthinal was evaporated under vacuum, and the dry residue was collected. The purity of the isolated pigment was checked by analytical HPLC (see Figure S1, Supporting Information). The sample was stored at −80 °C and then dissolved in either methanol (Sigma Aldrich, HPLC grade) or hexane (Sigma Aldrich, ACS grade) prior to the spectroscopic measurements.

Spectroscopy. All measurements were carried out at room temperature. Steady-state absorption spectra were obtained using a PerkinElmer Lambda 35 absorption spectrometer. Time-resolved measurements probing the 450−950 nm spectral range were performed using pulses with an ∼130 fs duration (average energy ∼1.9 mJ/pulse, peak wavelength ∼785 nm) obtained from a femtosecond laser system (Integra-I, Quantronix) operating at a repetition rate of 1 kHz. The output beam was divided into excitation and probe pulses. The desired wavelength of excitation pulses was achieved in an optical parametrical amplifier (TOPAS, Light Conversion). Probe pulses were led through a computer-controlled delay line and then focused onto a 2 mm sapphire plate to generate a white light continuum. Subsequently, the probe pulses were split into two beams, one overlapping with the pump pulse in the sample and the other serving as a reference. Both beams continued into the spectrograph where they were dispersed onto a dual diode-array detector consisting of 1024 elements (ExciPro, CDP Systems). The samples were held in a quartz rotating cuvette of 1 mm path length which ensured that each laser pulse interrogated a fresh volume of sample.

The time-resolved measurements in the 900−1200 nm range were carried out using the system based on a Ti:sapphire amplifier with a pulse stretcher and compressor (Spitfire-50, Spectra-Physics) pumped at a 1 kHz repetition rate by a Q-switched Nd:YLF laser (Evolution 15, Coherent) and seeded by pulses from a mode-locked Ti:sapphire oscillator (Tsunami, Spectra-Physics) pumped by a Nd:YVO_4 CW laser (Millenia, Spectra Physics). Output pulses having a wavelength of 800 nm, an energy of 600 μJ/pulse, a duration of ∼50 fs, and a 1 kHz repetition rate were split into two beams by a beam splitter, and 90% of the signal was sent to an optical parametric amplifier (OPA-800C, Spectra-Physics) to generate the pump beam. The remaining 10% was used to derive probe pulses. A white light continuum probe in the 900−1200 nm region was generated by a 3 mm sapphire plate. A 512 pixel array SU-LDV high-resolution InGaAs Digital Line Camera from Sensors Unlimited was used as a detector. The signals were averaged over 5 s. The samples were measured in a 2 mm cuvette and mixed continuously using a magnetic microstirrer to prevent photodegradation.

For both setups the integrity of the samples was checked by taking a steady-state absorption spectrum before and after every experiment. The intensity of the pump pulses was kept below 10^{15} photons $pulse^{-1}$ cm^{-2}. Mutual polarization between pump and probe beams was set at the magic angle (54.7°). All data from time-resolved measurements were fitted globally (DAFit, Pascher Instruments) to a sum of exponentials using a sequential kinetic scheme with increasing lifetimes.[52] The profile associated with each time step is denoted as an evolution-associated difference spectrum (EADS).

RESULTS

Steady-State Absorption Spectra. Steady-state absorption spectra of LH1−RC complexes from *Roseobacter* sp. COL2P and *Erythrobacter* sp. NAP1 and respective carotenoids in solution are shown in Figure 2. While the absorption bands corresponding to the Soret and Q_x bands of BChl-*a* had similar maxima in both species (372 and 590 nm in *Roseobacter* and 376 and 590 nm in *Erythrobacter*), the Q_y band of *Roseobacter* sp. COL2P was red-shifted (874 nm) compared to that in *Erythrobacter* sp. NAP1 (866 nm). This indicates differences in the interaction between the BChl-*a* and the protein as the position of the Q_y band is known to be very sensitive to the local environment of BChl-*a*.[53] Even larger differences were observed in the blue-green spectral region where the carotenoids absorb. Spheroidenone (Figure 1) bound to the *Roseobacter* LH1−RC complexes has an absorption maximum at 507 nm, whereas the absorption spectrum of spheroidenone is broad and featureless in methanol, which is typical of carbonyl carotenoids in polar solvents.[29,30] Upon binding to the LH1−RC complex the vibrational structure of the S_0−S_2 transition becomes evident. This is consistent with a reduction in conformational disorder in the protein where the carotenoid conformation is constrained within the binding pocket.

The LH1−RC complex from *Erythrobacter* sp. NAP1 binds two carotenoids, bacteriorubixanthinal and zeaxanthin (Figure 1), whose absorption bands can be identified in the absorption spectrum of *Erythrobacter* sp. NAP1 shown in Figure 2. Three distinct peaks at 438, 468, and 494 nm are associated with the vibrational bands of the S_0−S_2 transition of zeaxanthin, while the band around 540 nm is due to bacteriorubixanthinal. As

dx.doi.org/10.1021/jp309278y | J. Phys. Chem. B 2013, 117, 10987−10999

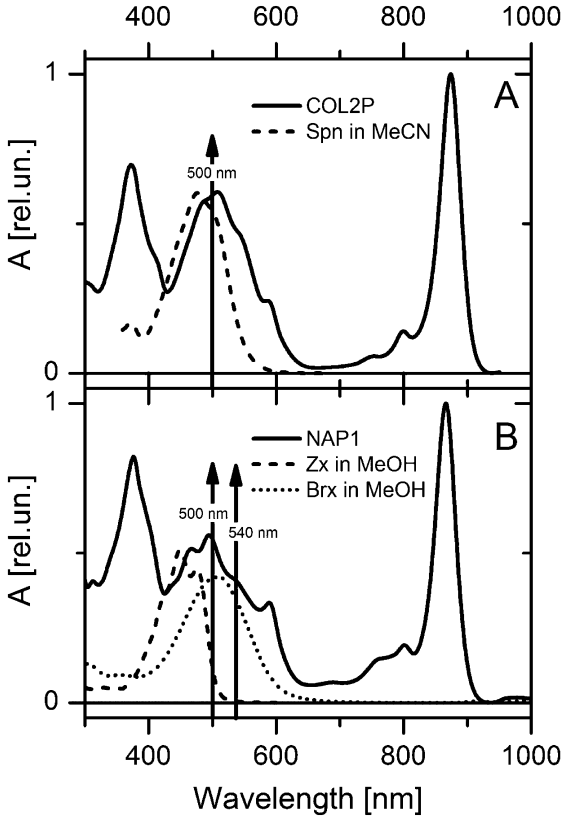

Figure 2. Absorption spectra of LH1−RC complexes from *Roseobacter* sp. COL2P (A) and *Erythrobacter* sp. NAP1 (B). Absorption spectra of respective carotenoids (Spn = spheroidenone, Zx = zeaxanthin, Brx = bacteriorubixanthinal) in acetonitrile (MeCN) or methanol (MeOH) are also shown along with the absorption spectra of LH1−RC complexes. Vertical arrows indicate excitation wavelengths used in time-resolved measurements.

seen for spheroidenone, the absorption spectrum of bacteriorubixanthinal, which has a conjugated carbonyl group, does not exhibit any vibrational structure when dissolved in a polar solvent. The weak absorption bands around 750 and 800 nm readily observable in the absorption spectra of both LH1−RC complexes are due to monomeric bacteriopheophytins and BChls, respectively, in the RC.[54]

Transient Absorption Spectra. *(a). Roseobacter sp. COL2P.* Transient absorption spectra of the LH1−RC complexes from *Roseobacter* sp. COL2P were recorded in both the visible (VIS) and near-infrared (NIR) spectral regions after excitation at 500 nm (Figure 3). In the VIS region, the early 150 fs spectrum shows a strong bleaching below 560 nm due to the S_0−S_2 transition of spheroidenone and excited-state absorption (ESA) above 560 nm associated with its S_1−S_N transition. Contrary to most other studies of carotenoids in light-harvesting complexes, the ESA signal extends far beyond the spectral region expected for an S_1−S_N transition. The ESA signal further increases above 700 nm and forms rather intense band peaking at ∼740 nm. This feature resembles the ICT band observed recently in the spheroidenone-containing LH1−RC−PufX complex from *Rba. sphaeroides*,[32] and its origin will be discussed in detail below. Besides the signals associated with spheroidenone, a slight dip around 580 nm due to Q_x bleaching, superimposed on the broad ESA signal from spheroidenone, can be observed in the 150 fs spectrum and becomes more noticeable at subsequent decay times, indicating

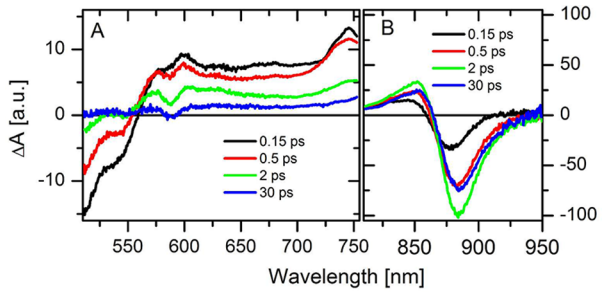

Figure 3. Transient absorption spectra of LH1−RC complexes from *Roseobacter* sp. COL2P recorded in the visible (A) and NIR (B) region after 500 nm excitation. The data are normalized to the number of photons in the excitation pulse to allow comparison of signal magnitudes in VIS and NIR regions.

an S_2-mediated channel exists for energy transfer from spheroidenone to BChl-*a*. It should be noted that at 500 nm direct excitation of BChl-*a* is negligible, so the observed Q_x bleaching must result from energy transfer from the S_2 state of spheroidenone. At longer delays, the intensity of spheroidenone-related features decreases, and the intensity of the Q_x bleaching at 590 nm increases due to an open energy transfer pathway between the carotenoid S_1 state and BChl-*a*. However, the Q_x bleaching is somewhat less intense in the spectrum recorded at 30 ps, and this is due to energy transfer from LH1 to RC.

To analyze carotenoid-to-BChl energy transfer in more detail, transient absorption spectra were recorded in the NIR region where BChl-*a* bleaching dominates. Figure 3B shows that BChl-*a* bleaching is present already at a time delay of 150 fs, confirming fast energy transfer from the S_2 state of spheroidenone. The bleaching becomes more pronounced at later delay times, consistent with additional excited BChl molecules being formed via the spheroidenone S_1 to BChl-*a* energy transfer pathway. Consequently, the magnitude of the Q_y bleaching decreases, in agreement with the occurrence of energy transfer from the LH1 antenna to the RC.

To obtain quantitative information about the excited state dynamics, global fitting analysis was performed. The resulting EADS are shown in Figure 4. In the case of the *Roseobacter* LH1−RC complex, four time constants were needed to obtain satisfactory fits in both the VIS and NIR regions. The first EADS (black) largely represents the spectrum of the excited S_2 state of spheroidenone and consists mainly of ground-state

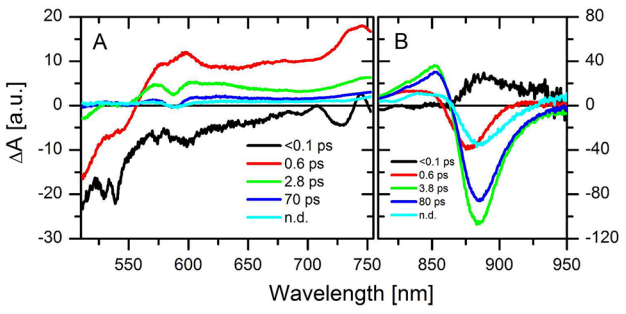

Figure 4. EADS resulting from global fitting analysis of data recorded in the visible (A) and NIR regions (B) after excitation of LH1−RC complexes of *Roseobacter* sp. COL2P at 500 nm. The data are normalized to the number of photons in the excitation pulse. n.d. = nondecaying component.

dx.doi.org/10.1021/jp309278y | *J. Phys. Chem. B* 2013, 117, 10987−10999

bleaching (GSB) and stimulated emission from the S_2 state. This component decays in less than 100 fs to form the second EADS (red) which is associated with the S_1 (weaker band at ~600 nm) and ICT states (stronger band at ~740 nm) in the VIS region and a characteristic BChl-*a* signal in the NIR at 875 nm. Thus, in both spectral regions the step associated with transformation of the first (black line in Figure 4) to the second (red line in Figure 4) EADS suggests active spheroidenone S_2-to-BChl-*a* energy transfer. The second EADS component evolves in 0.6 ps in both spectral regions into a third EADS component (green traces in Figure 4). This step is accompanied by the decay of the S_1 signal in the VIS and a significant increase of the BChl-*a* bleaching in the NIR, indicating a dominance of the spheroidenone S_1-to-BChl-*a* energy transfer pathway. We note that the 740 nm band assigned to the ICT state decays with the same time constant, suggesting that this state is involved in energy transfer. The third EADS decays in ~3 ps in both spectral regions to a fourth component (blue traces in Figure 4), but the decay of the spheroidenone signal is not accompanied by the onset of a feature belonging to BChl-*a*, so this step cannot be associated with energy transfer. The fourth EADS decays on a time scale of tens of picoseconds and reflects the energy transfer from LH1 into the RC, giving rise to EADS which do not decay within the temporal window of our experiment. Energy transfer from carotenoid S_1 to BChl-*a* is also confirmed by comparing kinetics at the maximum of spheroidenone S_1 ESA and at the BChl-*a* bleaching maximum (Figure S2, Supporting Information).

(b). Bacteriorubixanthinal in Solution. Whereas the excited-state properties of the two carotenoids, spheroidenone and zeaxanthin, found in the AAP LH1−RC complexes have been studied previously,[29,30,55−57] bacteriorubixanthinal, which occurs in the LH1−RC of *Erythrobacter* sp. NAP1, has never been examined by time-resolved spectroscopy. Knowledge of the excited-state dynamics of bacteriorubixanthinal in solution is important, given that it contains a conjugated carbonyl group (Figure 1). Thus, a polarity-induced effect on the excited-state spectra and dynamics might be expected, especially since the carbonyl group in bacteriorubixanthinal occurs as an aldehyde functional group, asymmetrically placed along the conjugated polyene chain.

Transient absorption spectra of bacteriorubixanthinal measured at 1 ps after excitation in *n*-hexane and methanol are compared in Figure 5. It is seen that in the nonpolar solvent, *n*-hexane, the transient absorption spectrum contains only features associated with the S_1-S_N transition peaking at 610 nm. However, when bacteriorubixanthinal is dissolved in the polar solvent, methanol, a broad ICT band appears in the 660−720 nm region. In contrast to carbonyl carotenoids such as spheroidenone[29,30] or echinenone[58] having a similar conjugation length, both of which exhibit weak ICT bands in polar solvents, the ICT band of bacteriorubixanthinal is of a magnitude comparable to that of the S_1-S_N transition. This indicates that the asymmetrically placed carbonyl group enhances the polarity-induced effect on the spectral line shape.

A comparison of the kinetics measured at 612 nm in the two solvents, methanol and *n*-hexane (inset of Figure 5), demonstrates that although the ICT state is more populated in methanol the solvent has essentially no effect on the lifetime of the S_1/ICT state. The state decays with the same time constant of 4.0 ± 0.3 ps. It is consistent with previous studies which have reported that for carbonyl carotenoids having the

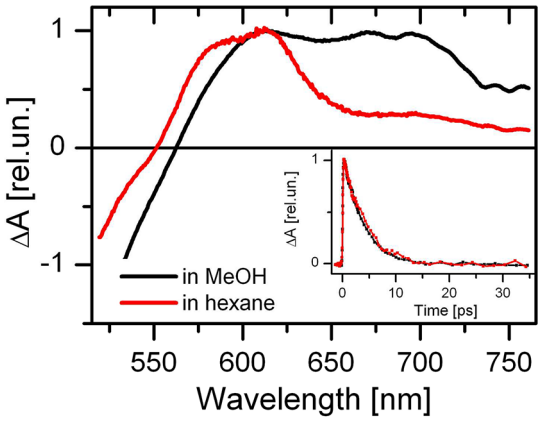

Figure 5. Transient absorption spectra of bacteriorubixanthinal in methanol (MeOH, black) and *n*-hexane (red) measured at 1 ps after excitation at 513 and 495 nm, respectively. Spectra are normalized to maximum. Inset: kinetics measured at 612 nm for bacteriorubixanthinal in methanol (black) and *n*-hexane (red). Kinetics are normalized to maximum.

S_1/ICT lifetimes in nonpolar solvents shorter than 10 ps there is no further change in the lifetime when the molecules are redissolved in polar solvents.[29,30,58] Yet, although the kinetics measured at 612 nm shown in the inset of Figure 5 are identical, global fitting of the entire spectral and temporal data sets reveals subtle differences between the data taken in the two solvents. EADS obtained from the global fitting analysis are shown in Figure S3 (Supporting Information). Whereas for bacteriorubixanthinal in *n*-hexane a single decay component with a time constant of 4.2 ps is sufficient to fit the data, an additional decay component is necessary to obtain a reasonable fit for the molecule dissolved in methanol; the data in methanol are best fit using two decay components of 1.1 and 3.7 ps. The amplitude of the first component is more pronounced in the spectral region of the ICT band, but the second dominates in the spectral region of the S_1-like transition (Figure S3B, Supporting Information). It should be noted that both components also have an amplitude in the S_2 bleaching region below 560 nm, implying that excited bacteriorubixanthinal in methanol returns to the ground state with two different time constants. This means that in methanol there are two populations of bacteriorubixanthinal, one with a 1.1 ps lifetime having a more pronounced ICT band and the other whose ICT band is weaker and decays to the ground state with a 3.7 ps time constant. This situation is reminiscent of the carbonyl carotenoid, hydroxyechinenone, bound to orange carotenoid protein (OCP) where two populations decaying with time constants of 0.9 and 3.3 ps were reported.[59,60] Thus, as it was suggested for hydroxyechinenone in OCP,[59] the two populations of bacteriorubixanthinal in methanol may differ in their configurations and/or hydrogen bonding to the carbonyl group.

(c). Erythrobacter sp. NAP1. VIS and NIR transient absorption spectra of the LH1−RC complexes of *Erythrobacter* sp. NAP1 are shown in Figure 6. To separately interrogate the different excited-state properties of bacteriorubixanthinal and zeaxanthin in the LH1−RC complex, two different excitation wavelengths, 540 and 500 nm, were used. The wavelength 540 nm excites almost exclusively bacteriorubixanthinal, whereas 500 nm excites both carotenoids in the LH1−RC complex (Figure 2). Comparing the VIS transient absorption spectra of

dx.doi.org/10.1021/jp309278y | J. Phys. Chem. B 2013, 117, 10987−10999

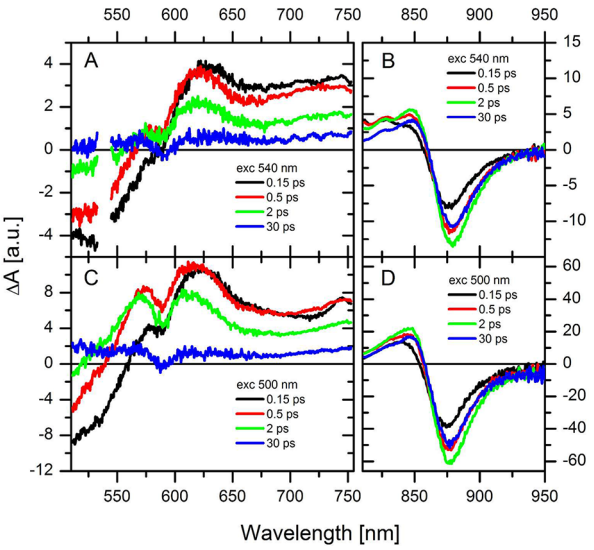

Figure 6. Transient absorption spectra of LH1−RC complexes from *Erythrobacter* sp. NAP1 recorded in the visible (A, C) and NIR regions (B, D) after excitation at 540 nm (A, B; only bacteriorubixanthinal is excited) and 500 nm (C, D; bacteriorubixanthinal and zeaxanthin are excited). The data are normalized to the number of photons in the excitation pulse.

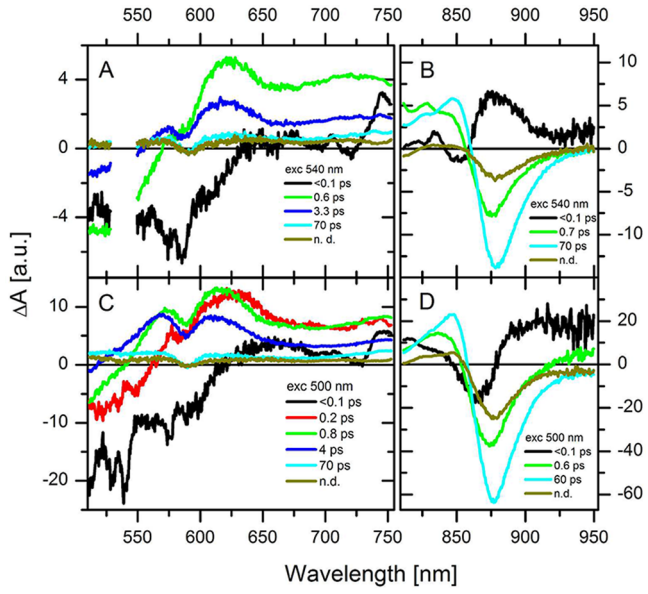

Figure 7. EADS resulting from global fitting analysis of data recorded in the visible (A, C) and NIR regions (B, D) after excitation of LH1−RC complexes of *Erythrobacter* sp. NAP1 at 540 nm (A, B; only bacteriorubixanthinal is excited) and 500 nm (C, D; bacteriorubixanthinal and zeaxanthin are excited). The data are normalized to the number of photons in the excitation pulse. n.d. = nondecaying component.

Erythrobacter sp. NAP1 recorded using the different excitations (Figures 6A and C), the overall shape of the transient absorption spectrum was very similar above ∼590 nm. Thus, the ESA band peaking at 625 nm can be attributed to the S_1−S_N transition of bacteriorubixanthinal. However, the band with a maximum near 575 nm (Figure 6C), which occurred only when 500 nm excitation was used, can be unequivocally identified as due to the S_1−S_N ESA band of zeaxanthin. Other spectral features were similar to those in LH1−RC from *Roseobacter* sp. COL2P, including the 740 nm band tentatively assigned to the ICT state, which in the *Erythrobacter* LH1−RC complex originates most likely from bacteriorubixanthinal.

A comparison of the NIR transient absorption spectra measured after 540 and 500 nm excitation did not reveal any significant differences in the Q_y bleaching dynamics (Figures 6B and D). This suggests that the role of zeaxanthin in energy transfer to BChl-*a* is negligible because excitation of zeaxanthin at 500 nm did not affect the rise of the BChl-*a* bleaching band that would be expected in the case of energy transfer from zeaxanthin excited at 500 nm. To separate the two carotenoids, a global analysis of the spectral and temporal data sets was carried out.

The global fitting analysis was carried out in the VIS and NIR regions after excitation at both 540 and 500 nm (Figure 7). To fit the VIS spectra generated by excitation at 540 nm (Figure 7A), four components were needed with time constants similar to those obtained for the *Roseobacter* LH1−RC complex. The S_2-mediated energy transfer is confirmed in *Erythrobacter* sp. NAP1 by the presence of bleaching of the BChl-*a* Q_x band in the second EADS in the VIS (green trace in Figure 7A) and bleaching of the BChl-*a* Q_y band in the NIR (green trace in Figure 7B). The second EADS, having all the characteristics of the S_1 state with some ICT character, decays in 0.6 ps in the VIS region. A comparable time component (0.7 ps), showing a further increase of the BChl-*a* bleaching in NIR, clearly demonstrates energy transfer between the S_1 state of bacteriorubixanthinal and BChl-*a*. In contrast to the results obtained from the *Roseobacter* LH1−RC complex, a satisfactory global fit of the data sets from *Erythrobacter* LH1−RC in the NIR required only three time constants. The ∼3−4 ps time component was absent, suggesting that the 3.3 ps component observed in the VIS most likely originated from carotenoids rather than BChls. Indeed, as bacteriorubixanthinal in methanol has a decay component of 3.7 ps and is associated with the S_1/ICT lifetime (see above), the 3.3 ps time component may be ascribed to bacteriorubixanthinal molecules that do not transfer energy to BChl-*a*. The final component (neglecting the nondecaying component) occurs on a time scale of tens of picoseconds and, as above, is due to energy transfer to the RC.

Analysis of the 500 nm excitation data (Figure 7C, D) is more complicated due to the involvement of zeaxanthin. The participation of this second carotenoid required an additional time constant of 0.2 ps to fit the data in the VIS region (red trace in Figure 7C). The data show that within 0.2 ps zeaxanthin S_1 to S_N absorption appears. Thus, the time constant represents the S_2 lifetime of zeaxanthin in LH1−RC *Erythrobacter* sp. NAP1. Because this is similar to the S_2 lifetime of zeaxanthin measured in solution,[61] it rules out any significant contribution of the zeaxanthin S_2 state to energy transfer to BChl-*a* in this preparation. Apart from the appearance of the ESA band around 575 nm (Figure 7C), excitation of zeaxanthin has essentially no effect on either the time constants of the excited-state processes or the shape of the EADS in the VIS region. Also, the EADS and time constants obtained from the NIR data sets generated using 500 nm excitation (Figure 7D) remain virtually unchanged compared to those obtained using excitation at 540 nm (Figure 7B). This confirms that there is negligible involvement of zeaxanthin in carotenoid-to-BChl-*a* energy transfer in LH1−RC complexes of *Erythrobacter* sp. NAP1. The energy transfer processes in *Erythrobacter* sp. NAP1 are visualized in Figure S4 (Supporting Information) that shows kinetics of carotenoid bleaching in

dx.doi.org/10.1021/jp309278y | J. Phys. Chem. B 2013, 117, 10987−10999

LH1−RC and in solution accompanied by the BChl-*a* bleaching kinetics. While kinetics after bacteriorubixanthinal excitation (Figure S4A, Supporting Information) confirm its involvement in energy transfer, kinetics recorded after zeaxanthin excitation (Figure S4B, Supporting Information) do not show any signs of energy transfer from zeaxanthin.

Probing in the 900−1200 nm Spectral Region. To search for the possible presence of signals associated with the formation of carotenoid radicals, we have extended our transient absorption measurements into the 900−1200 nm region. Previous reports on LH2 complexes have shown that upon direct excitation of the carotenoid bound in the LH2 pigment−protein complex a fraction of the S_2 population is depopulated through electron transfer to BChl-*a* and results in the formation of a short-lived (<10 ps) carotenoid cation radical.[51,62,63] The biological function of this process is unknown, although it could be a mechanism by which photoprotection is afforded to the LH2 complex by removing excess carotenoid excitations from the system. Carotenoid radicals are readily identified by their D_0−D_2 transition that has a maximum absorption between 900 and 1100 nm depending on the π-electron conjugation length of the molecule.[64]

Transient absorption spectra of both AAP LH1−RC complexes were measured in the 900−1200 nm region (Figure 8). Immediately after excitation, the transient absorption spectrum of *Roseobacter* sp. COL2P (black trace in Figure 8A) is dominated by a signal that is due to ESA from the S_2 state of spheroidenone. This is documented by the comparison of the signal with S_2 ESA from spheroidenone-containing LH2.[51] A similar signal was observed for *Erythrobacter* sp. NAP1 excited at 500 nm (black trace in Figure 8C). Thus, the signal at 0 ps corresponds to the ESA from the S_2 state of zeaxanthin. No such band was detected when *Erythrobacter* sp. NAP1 was excited at 540 nm (black trace in Figure 8B), indicating that the transition from the bacteriorubixanthinal S_2 state has minimal ESA signal in this spectral region.

In *Erythrobacter* sp. NAP1, the transient absorption spectrum recorded at delay times of 0.5 and 10 ps (Figure 8) did not change and did not exhibit any bands attributable to carotenoid radicals. The broad positive signal beyond 1000 nm is due to ESA of BChl-*a* that has also been reported previously in LH2 complexes.[51,62] The transient absorption spectrum of the *Roseobacter* sp. COL2P LH1−RC complex recorded at a 0.5 ps delay (red trace in Figure 8A) has a distinct band centered at 960 nm that is remarkably similar to the band observed in spheroidenone-containing complexes from the LH2 complex from *Rba. sphaeroides*[51] and from the LH4 complex from *Roseobacter denitrificans*.[50] These reports assigned this band to a spheroidenone cation radical. Global fitting of the *Roseobacter* sp. COL2P data, which is shown in the Supporting Information (Figure S5), demonstrates that the 960 nm band decays with a 0.7 ps time constant. This is very close to the 0.6 ps lifetime reported by Cong et al.[51] and the 0.75 ps lifetime reported by Niedzwiedzki et al.[50] This agreement suggests that a spheroidenone cation radical may also be generated in the *Roseobacter* sp. COL2P LH1−RC complex. Alternatively, the 960 nm ESA band shown in Figure 8A may be associated with the ICT state of spheroidenone that has been reported to exhibit weak stimulated emission around 1000 nm in solution.[30] In this case, the shape of the transient absorption spectrum at 0.5 ps (red trace in Figure 8A) may be explained as a negative signal due to ICT stimulated emission peaking around 1000 nm superimposed on a broad featureless ESA of BChl-*a*. This explanation is made more plausible by the fact that the 0.7 ps time constant associated with decay of the 960 nm band (Figure S5, Supporting Information) is close to the lifetime of the S_1/ICT state of spheroidenone in *Roseobacter* complexes (Figure 4A). The absence of this feature in *Erythrobacter* sp. NAP1 would then be attributable to a weaker ICT band in the LH1−RC complex from this species—the intensity of the stimulated emission is so weak that it is not detectable with the the present S/N ratio.

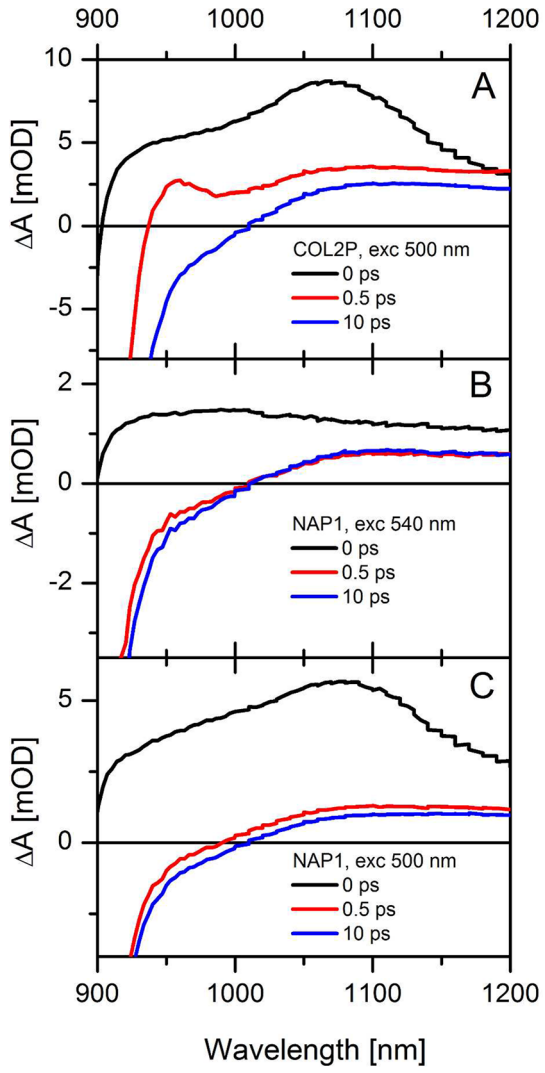

Figure 8. Transient absorption spectra of LH1−RC complexes of *Roseobacter* sp. COL2P (A) and *Erythrobacter* sp. NAP1 (B, C) in the carotenoid radical region. The excitation wavelengths are indicated in the figure.

DISCUSSION

The present results clearly show that both LH1−RC complexes exhibit efficient energy transfer between carotenoids and BChl-*a*. The carotenoid composition of the LH1−RC complexes from AAPs allows a direct comparison with their purple nonsulfur bacterial counterparts because the *Roseobacter* sp. COL2P LH1−RC complex contains the carotenoid spheroidenone which also occurs in the LH1 and LH2 complexes of purple nonsulfur bacteria. On the other hand, the LH1−RC complex from *Erythrobacter* sp. NAP1 contains bacteriorubixanthinal, a carotenoid that has not been characterized by

dx.doi.org/10.1021/jp309278y | J. Phys. Chem. B 2013, 117, 10987−10999

ultrafast time-resolved spectroscopy, and zeaxanthin which occurs typically in Chl-*a* based light-harvesting systems. Thus, the *Erythrobacter* sp. NAP1 LH1−RC complex provides a unique opportunity to test the light-harvesting ability of bacteriorubixanthinal which has an unusual structure (Figure 1) and zeaxanthin whose excited-state properties have never been characterized in a light-harvesting system containing BChl-*a*. Moreover, transient absorption spectra of both LH1−RC complexes exhibit a spectral feature at ∼740 nm that was recently identified in the spheroidenone-containing LH1−RC−PufX complex from *Rba. sphaeroides* as being due to the ICT state of spheroidenone.[32]

Origin of the 740 nm Band. On the basis of the similarity of the transient absorption band around 740 nm in *Roseobacter* sp. COL2P with a similar spectral feature observed in LH1−RC−PufX complexes of *Rba. sphaeroides* containing a carbonyl carotenoid spheroidenone (Figure S6, Supporting Information), we propose that the band is associated with an ICT−S_n transition. This transition, which is typically red-shifted from the S_1 to S_N band, is characteristic of carotenoids having a conjugated carbonyl group,[29,30] and its magnitude is correlated with a degree of asymmetry introduced by the conjugated carbonyl group.[58,65,66] Carbonyl carotenoids with one conjugated carbonyl group attached to a short C═C conjugated backbone exhibit a strong ICT band,[29,30] and the magnitude of the ICT band increases with decreasing conjugation length.[65] For carotenoids with two carbonyl groups positioned symmetrically, a very weak or no ICT band is observed.[66] The band is also very weak for carotenoids having one carbonyl group if it is attached to a long ($N > 10$) conjugated chain.[58] Included in this latter group is spheroidenone which has only a weak ICT band even in the very polar solvents, methanol or acetonitrile.[29,30]

To explain the appearance of the ICT band of spheroidenone in the LH1−RC complex from *Roseobacter* sp. COL2P, we propose that the binding cleft of spheroidenone twists the C═O group into the s-trans configuration, while the s-cis configuration is the most stable spheroidenone structure in solution.[32] This is supported by previous ultrafast time-resolved spectroscopic studies of hydroxyechinenone, which upon binding to the Orange Carotenoid Protein (OCP) exhibited an ICT ESA band. No such band was observed in solution.[59] The argument that the s-trans configuration is necessary to generate the ICT band is also supported by the X-ray structure of OCP,[67] which shows that the carbonyl group of hydroxyechinenone is in s-trans configuration. On the basis of the similarity in the transient absorption spectra of the LH1−RC complex from *Roseobacter* sp. COL2P and the LH1−RC−PufX from *Rba. sphaeroides* containing spheroidenone (Figure S6, Supporting Information), we conclude that the same mechanism of ICT activation occurs in both systems and suggest that the carotenoid binding cleft for the carotenoid in *Roseobacter* LH1−RC complexes has the same structure as that in purple nonsulfur bacteria.

The presence of the ICT band in the LH1−RC complex of *Roseobacter* sp. COL2P can thus be explained by the same mechanism as described for the LH1−RC−PufX complex from *Rba. sphaeroides*, as both complexes contain the same carotenoid, spheroidenone. The appearance of the ICT band in the LH1−RC complex from *Erythrobacter* sp. NAP1, which contains bacteriorubixanthinal and zeaxanthin, must be of a different origin. Since it is known that a necessary condition for the ICT band to appear is a conjugated carbonyl group, for the LH1−RC complex from *Erythrobacter* sp. NAP1 it must be the bacteriorubixanthinal that is responsible for the presence of the ICT band. However, bacteriorubixanthinal has the carbonyl group attached as an aldehyde off the main conjugated chain (Figure 1). Thus, the mechanism of linearization of the conjugated chain by twisting the C═O group into an s-trans configuration as proposed for spheroidenone is not applicable for bacteriorubixanthinal. Instead, the presence of the ICT band due to bacteriorubixanthinal in the LH1−RC complex from *Erythrobacter* suggests that the carbonyl group of the carotenoid is sequestered in a polar environment. This is because the magnitude of the ICT band observed in the pigment−protein complex is comparable to that observed for bacteriorubixanthinal in methanol (compare Figures 5 and 6).

To further support the conclusion that the 740 nm band is due to the ICT state, Figure 9 compares the kinetics measured at the maxima of the S_1−S_N and ICT−S_n transitions of the carotenoids in the LH1−RC complexes from both species. It is assumed that the S_1 and ICT states are strongly coupled[30,48,68]

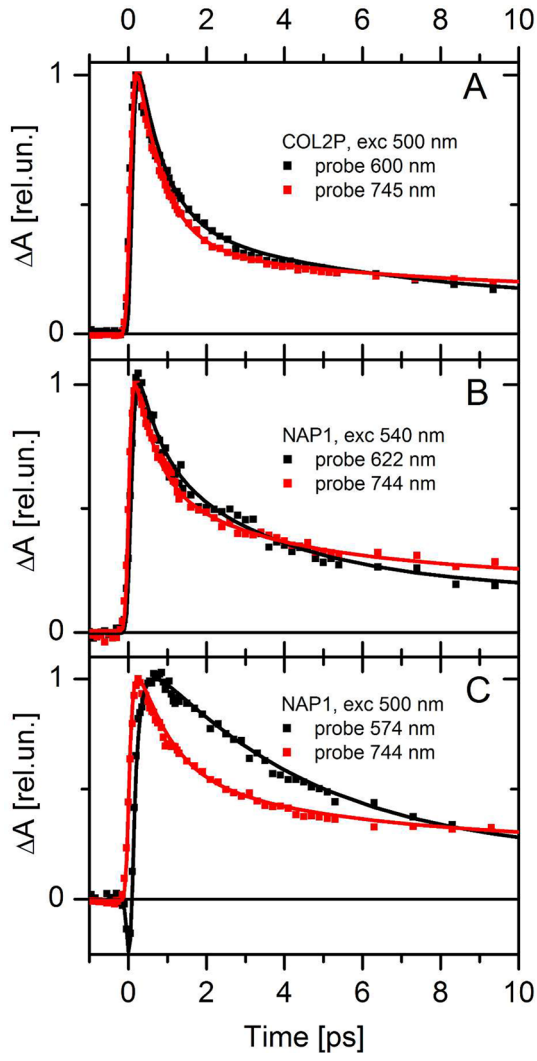

Figure 9. Comparison of kinetics measured at the maxima of the S_1-like and ICT-like bands for *Roseobacter* sp. COL2P (A) and *Erythrobacter* sp. NAP1 (B, C). (A) Spheroidenone S_1 (black) and ICT (red). (B) Bacteriorubixanthinal S_1 (black) and ICT (red). (C) Zeaxanthin S_1 (black) and ICT (red). Excitation wavelengths are indicated in the figure. Kinetics are normalized to their maxima.

and in light-harvesting complexes are usually considered as a single excited state denoted S_1/ICT.[20,34,35] Although the details of this coupling are still unclear, its major consequence is that both S_1-like and ICT-like bands in the transient absorption spectra exhibit nearly identical dynamics.[30,47,48,68,69] Thus, if the 740 nm band is due to an ICT-like transition, it should decay with the same time constant as the S_1-S_N signal. Direct comparison of kinetics in Figure 9 shows that decay of the 740 nm band (probed at 744 or 745 nm) is virtually identical to that measured both at 600 nm in *Roseobacter* (spheroidenone S_1-S_N transition, Figure 9A) and at 622 nm in *Erythrobacter* LH1-RC (bacteriorubixanthinal S_1-S_N transition, Figure 9B). On the other hand, the kinetics at 574 nm (zeaxanthin S_1-S_N transition, Figure 9C) obtained after excitation of *Erythrobacter* LH1-RC at 500 nm are markedly different compared to those probed at 744 nm recorded after the same excitation. It is therefore clear that the decay of the 740 nm band matches the decay of the S_1-S_N signal of the carbonyl carotenoids, spheroidenone and bacteriorubixanthinal, both of which have carbonyl groups, while for the noncarbonyl carotenoid zeaxanthin no agreement is observed. Thus, based on this evidence we conclude that the 740 nm band is associated with the ICT state of carbonyl carotenoids. Since the decays of the ICT and S_1 bands are accompanied by a rise in the BChl-*a* bleaching in the NIR spectral region (Figures 4 and 7), this implies that the ICT state is directly involved in carotenoid-to-BChl-*a* energy transfer. The donor state is denoted S_1/ICT according to the previously established notation.

Carotenoid-to-BChl-*a* Energy Transfer. Figures 4 and 7 show clearly that energy is transferred from the carotenoids to BChls from both the S_2 and S_1/ICT states of spheroidenone and bacteriorubixanthinal. Although a quantitatively precise measurement of the S_2-mediated energy transfer rate is not possible due to insufficient time resolution of our spectrometer, comparing the "fast" and "slow" phases of the BChl-*a* rise (Figures 4 and 7) indicates that the S_2 channel is important in the LH1−RC complex from *Erythrobacter* sp. NAP1 where as much as 50% of the BChl-*a* rise occurs within 100 fs. This channel is less important in the LH1−RC complex from *Roseobacter* sp. COL2P where its contribution does not exceed 30%.

A more precise analysis can be done for the S_1/ICT-mediated pathway. The S_1/ICT state is depopulated via internal conversion to the S_0 state, with a rate constant denoted $k_1 = \tau_1^{-1}$, and via energy transfer to BChl-*a* with a rate constant denoted k_{ET}. Using the relation $k = k_1 + k_{ET}$, where k is the rate constant for the S_1/ICT state depopulation in LH1−RC complexes obtained from experiment, k_{ET} can be calculated. Furthermore, the efficiency of energy transfer via the S_1/ICT state, Φ_{ET}, can be calculated from the expression

$$\Phi_{ET} = k_{ET}/(k_{ET} + k_1) = 1 - \tau/\tau_1$$

Whereas this calculation of energy transfer efficiency is straightforward for noncarbonyl carotenoids whose S_1 lifetimes are independent of the polarity of the environment, for carbonyl carotenoids it poses a challenge because their S_1/ICT lifetimes depend on this factor.[29,30] Consequently, their intrinsic S_1/ICT lifetime in the absence of energy transfer in light-harvesting complexes is not known. Yet, for spheroidenone, no polarity dependence of the dynamics of the S_1/ICT state was observed; its S_1/ICT lifetime is 6 ps regardless of the solvent polarity.[29,30] Therefore, this value may be used for the intrinsic S_1/ICT lifetime of spheroidenone in the LH1−RC complex from *Roseobacter* sp. COL2P.

Assuming that the S_1/ICT lifetime of spheroidenone τ is 0.6 ps (Figure 4A) in the LH1−RC complex from *Roseobacter* sp. COL2P and taking τ_1 = 6 ps, we obtain an energy transfer time of τ_{ET} = 0.67 ps, which corresponds to an efficiency of the S_1/ICT channel of 90%. In this analysis, however, linearization of the conjugated chain caused by twisting the C═O group into s-trans configuration[32] was not taken into account. Linearization is expected to shorten the intrinsic S_1/ICT lifetime. This is observed for hydroxyechinenone whose lifetime is reduced from 6 ps in solution to 3 ps in the OCP complex.[59] The protein binding site forces the end ring containing carbonyl group into s-trans configuration, and because OCP contains carotenoid as the only bound pigment, the shortening of the S_1/ICT lifetime is solely due to the structural change of the carotenoid. Thus, shortening of the intrinsic S_1/ICT lifetime is also expected for spheroidenone in LH1−RC complexes. If it is assumed that the carbonyl group is attached in an s-trans configuration with the main conjugation consisting of 10 C═C bonds, this would render the effective conjugation of spheroidenone the same as for a linear carotenoid having N = 11 (e.g., lycopene). In this case, its intrinsic S_1/ICT lifetime should be around 4 ps,[56,70,71] and the energy transfer time would be τ_{ET} = 0.71 ps, which would drop the energy transfer efficiency only slightly to 85%.

In the case of the *Erythrobacter* LH1−RC complex, the situation is more complicated because we have no reference to estimate the intrinsic S_1/ICT lifetime of bacteriorubixanthinal. In solution, the S_1/ICT lifetime of bacteriorubixanthinal is ∼4 ps, but an additional ∼1 ps component is observed in methanol (Figure S3, Supporting Information) and is most likely associated with a specific configuration and/or hydrogen bonding of the solvent to the carbonyl group of the molecule. Lacking any information about the configuration of bacteriorubixanthinal in LH1−RC, we will assume that the two lifetimes, 1.1 and 3.7 ps, obtained from the global fitting analysis of the data set taken in methanol, are limiting values for calculation of the energy transfer times. Then, taking the 3.7 ps value as the upper limit for the intrinsic S_1/ICT lifetime of bacteriorubixanthinal in the LH1−RC complex, and using the value of 0.6 ps as the measured S_1/ICT lifetime (Figure 7A), we obtain values of 0.72 ps and 84% for τ_{ET} and Φ_{ET}, respectively. Taking the value of 1.1 ps as the lower limit for the intrinsic S_1/ICT lifetime of bacteriorubixanthinal, we obtain values of 1.3 ps and 45% for the energy transfer time and efficiency, respectively.

Thus, although we cannot determine the actual intrinsic S_1/ICT lifetimes of spheroidenone and bacteriorubixanthinal in the LH1−RC complexes, reasonable estimates give efficiencies of the S_1/ICT channel in the 85−90% range for spheroidenone in the LH1−RC complex of *Roseobacter* sp. COL2P and 45−84% for bacteriorubixanthinal in the LH1−RC complex of *Erythrobacter* sp. NAP1. For spheroidenone, this efficiency is slightly larger than that obtained for spheroidenone in the LH2 complex from purple nonsulfur bacteria, which has efficiency values in the range 76−87%.[51,62] Since no ICT state was observed for spheroidenone in the LH2 complex,[51,62] it is tempting to conclude that populating the ICT state of spheroidenone does not have a significant impact on the carotenoid-to-BChl-*a* energy transfer efficiency. However, taking into account the proposed linearization of spheroidenone in the LH1−RC which extends its effective conjugation to approximately 11,[32] an efficiency larger than 80% would be

rather unusual. Noncarbonyl carotenoids with N = 11 such as lycopene or rhodopin glucoside have a very low efficiency of the S_1 channel in LH2.[10,11,70] The same conclusion was reached for LH1 complexes reconstituted with lycopene, a noncarbonyl carotenoid of comparable conjugation length.[33] This underscores the importance of populating the ICT state in LH1−RC complexes having spheroidenone to promote carotenoid-to-BChl-*a* energy transfer.

The key role of the ICT state in enhancing the energy transfer efficiency is also clear in the LH1−RC complex of *Erythrobacter* sp. NAP1. Bacteriorubixanthinal has an S_1/ICT lifetime of ∼4 ps in solution, indicating its effective conjugation length is $N \sim 11$; linear carotenoids with N = 11 (lycopene) and N = 12 (rhodovibrin) have S_1 lifetimes of 4 and 2.7 ps, respectively.[24,71,72] Thus, without coupling to the ICT state, bacteriorubixanthinal should have only negligible participation of the S_1 channel in energy transfer, as is the case for noncarbonyl carotenoids with N = 11−12 in LH2 and LH1 complexes.[10,24,33,51] Yet, the efficiency of the S_1/ICT channel in the LH1−RC complex of *Erythrobacter* sp. NAP1 is at least 45%. This must be due to the population of the ICT state which both enhances the donor−acceptor coupling[20] and optimizes spectral overlap by making the S_1/ICT energy slightly higher than for noncarbonyl carotenoids having comparable conjugation lengths.[30]

Finally, the role of zeaxanthin in the *Erythrobacter* sp. NAP1 LH1−RC complexes should be discussed. From Figure 7C it follows that the zeaxanthin S_1−S_N ESA band appears with ∼0.2 ps which is a time constant that is not matched with a rise of BChl-*a* bleaching. This eliminates the involvement of the zeaxanthin S_2 state in carotenoid-to-BChl-*a* energy transfer. Similarly, the S_1−S_N band of zeaxanthin decays with a 4 ps time constant in the *Erythrobacter* LH1−RC complex, and no corresponding rise component is observed for BChl-*a* in the NIR spectral region (Figure 7D). Interestingly, the reported value of the zeaxanthin S_1 lifetime in solution is ∼9 ps,[55−57] which is significantly longer than the S_1 lifetime measured in the LH1−RC complex. Since the 4 ps time constant is not reflected in the BChl bleaching signal, the shortening of the S_1 lifetime in the protein cannot be due to energy transfer. Instead, this result suggests that the zeaxanthin S_1 lifetime is different in the *Erythrobacter* LH1−RC complex from its value in solution. It must be noted, however, that the global analysis of the data taken using 500 nm excitation and fitted to a sequential model may lead to an error in the S_1 lifetime of zeaxanthin in the *Erythrobacter* sp. NAP1 LH1−RC complex. This is because the S_1 state of zeaxanthin clearly decays independently of bacteriorubixanthinal in the complex. Thus, fitting the data to a sequential model may artificially shorten the S_1 lifetime of zeaxanthin by mixing it with the lifetime associated with the bacteriorubixanthinal decay (Figure 7C). Therefore, the kinetics of the S_1−S_N ESA signal from zeaxanthin was fitted separately using a single wavelength analysis. The resulting fit required two decay components of 2.5 ps (41%) and 7.5 ps (46%), with the remaining 13% accounting for the nondecaying component due to BChl-*a*. While the 2.5 ps component is similar to the value of 3.3 ps obtained upon selective excitation of bacteriorubixanthinal at 540 nm (Figure 7A) and thus unrelated to zeaxanthin, the 7.5 ps component should correspond to the S_1 lifetime of zeaxanthin. This demonstrates that the zeaxanthin lifetime could be longer than the 4 ps value extracted from the global fitting, but even the 7.5 ps lifetime obtained from the single wavelength fitting is slightly shorter than the zeaxanthin S_1 lifetime of 9 ps in solution, suggesting once again that the binding site of the LH1−RC complex alters excited-state properties of the carotenoid. While this effect might be considered unusual for linear carotenoids, it is not for carotenoids having conjugation extended to terminal rings. It may easily happen that binding to the protein twists the terminal rings in such a way that the effective conjugation length of the molecule is extended and consequently leads to a shorter S_1 lifetime. Thus, it is possible that one (or both) of the terminal rings of zeaxanthin is twisted into to an s-trans configuration or simply planarized upon binding to the LH1−RC complex in *Erythrobacter* sp. NAP1. This hypothesis is reminiscent of the twisting of the carbonyl group of spheroidenone in *Roseobacter* sp. COL2P and in the LH1−RC−PufX complex from *Rba. sphaeroides*.[32] Since zeaxanthin in the LH1−RC complex from *Erythrobacter* sp. NAP1 does not transfer energy to BChl-*a*, its role is most likely photoprotective. Then, as suggested for spheroidenone, the hypothesized twisting of the zeaxanthin terminal ring(s) would lead to a longer effective conjugation, modulating the triplet state energy to optimize quenching of singlet oxygen and/or BChl-*a* triplets.[32]

Origin of the ∼3 ps Time Constant. The global analysis revealed time constants of ∼3 ps for both LH1−RC complexes in the visible region (Figures 4A, 7A, and 7C). In the LH1−RC complex from *Roseobacter* sp. COL2P, a time constant of 3.8 ps was also obtained from the data set taken in the NIR region, but since it corresponds to the decay of Bchl-*a* bleaching, it cannot be due to energy transfer. Instead, this indicates that this component is probably associated with the dynamics of BChl-*a*. This conclusion is also supported by the fact that the 2.8 ps EADS component in the visible region differs markedly from that corresponding to the carotenoid S_1/ICT state. It resembles the ESA signal of excited BChl-*a* as evidenced by data obtained from direct excitation of BChl-*a* at 866 nm (Figure S7, Supporting Information). However, a minor contribution of spheroidenone to the 2.8 ps EADS component cannot be ruled out because a weak bleaching signal is seen in the short wavelength portion of the 2.8 ps EADS profile (Figure 4A). Thus, we conclude that in the LH1−RC complex from *Roseobacter* sp. COL2P the ∼3 ps component is due predominantly to BChl-*a* dynamics, with a minor contribution from spheroidenone that must be due to molecules that do not transfer energy to BChl-*a*. This provides additional evidence that the intrinsic S_1/ICT lifetime of spheroidenone in the LH1−RC complex from the *Roseobacter* sp. COL2P complex is substantially shorter than the 6 ps recorded in solution,[29,30] further supporting the idea that linearization of the carotenoid backbone upon binding to the protein shortens the intrinsic S_1/ICT lifetime.

The situation is different in the LH1−RC complex from *Erythrobacter* sp. NAP1, where the ∼3 ps time constant was found exclusively in the data taken in the visible spectral region (Figure 7). Furthermore, the visible spectrum contains typical carotenoid-related features (ESA around 575 and 620 nm associated with zeaxanthin and bacteriorubixanthinal, respectively). The time constants of 3.3 (excitation at 540 nm) and 4 ps (excitation at 500 nm) are close to the S_1/ICT lifetime of bacteriorubixanthinal in solution (Figure S3, Supporting Information), corroborating the relation of the EADS components (blue traces in Figures 7A and C) with carotenoids that do not transfer energy to BChl.

Although the explanation of the ~3 ps component as being due to carotenoids unable to transfer energy to BChl is plausible, it is not easy to imagine their position in the (almost) circularly symmetrical LH1−RC complex. The LH1 complex either forms an incomplete ellipse with 15 $\alpha\beta$ subunits surrounding the RC,[31] each subunit incorporating two BChls and one[73] or two[74] carotenoids, or it could be a closed ellipse with 16 $\alpha\beta$ subunits either in the monomeric form[75] or in the form of S-shaped dimers[76] with 14 subunits per monomer, interconnected by the PufX protein.[77] The structure of LH1−RC complexes from AAPs is unknown, but both strains studied here lack the PufX protein, suggesting that LH1−RC complexes of these AAP strains might form monomeric units. Yet, it is possible that orientations of carotenoids in the binding sites of an $\alpha\beta$ subunit may differ, leading to distinct carotenoid−BChl-*a* energy transfer efficiencies.

CONCLUSIONS

In this work we compared the excited-state dynamics and energy transfer properties in LH1−RC complexes from two AAPs having different carotenoid compositions. While the complex from *Roseobacter* sp. COL2P contains only a single carotenoid, spheroidenone, the LH1−RC complex from *Erythrobacter* sp. NAP1 binds two carotenoids, bacteriorubixanthinal and zeaxanthin. In both complexes, the carotenoids transfer energy to BChl-*a* from both the S_2 and S_1 states as depicted in the scheme shown in Figure 10. In both LH1−RC complexes, conjugated carbonyl groups of spheroidenone or bacteriorubixanthinal lead to the population of the ICT state. Spheroidenone exhibits a strong ICT ESA band despite the lack of such a band even in most polar solvents. This indicates that the ICT state in the LH1−RC complex from the *Roseobacter* sp. COL2P complex is activated by a structural change of spheroidenone facilitated by the carotenoid binding site. This is similar to a recent report on the spheroidenone-binding LH1−RC−PufX complex from *Rba. sphaeroides*.[32] In *Erythrobacter* sp. NAP1, the ICT band of bacteriorubixanthinal is comparable in intensity to that observed for bacteriorubixanthinal in methanol, suggesting that the carbonyl group of this carotenoid in the LH1−RC complex is sequestered in a polar binding site. Most importantly, the population of the ICT state in both complexes promotes efficient energy transfer via the coupled S_1/ICT state. This ICT-mediated enhancement of the S_1-channel for energy transfer to BChl-*a* is only moderate for spheroidenone in the LH1−RC complex from *Roseobacter* sp. COL2P compared to the same channel in the LH2 complex from *Rba. sphaeroides* where the ICT state of spheroidenone remains inactive upon binding.[51,62] In the LH1−RC complex from *Erythobacter* sp. NAP1, however, the enhancement of energy transfer via the S_1-channel due to coupling with the ICT state is significant. This is because noncarbonyl carotenoids having comparable conjugation lengths have the S_1 channel largely suppressed.[11,33,51]

Opening of the S_1 channel is achieved via S_1/ICT coupling which is thought to modulate the S_1/ICT energy; carbonyl carotenoids usually have their S_1/ICT state higher than their noncarbonyl counterparts.[30] Thus, activation of the ICT state of spheroidenone and bacterioruboxanthinal in the LH1−RC complex not only enhances donor−acceptor coupling but also optimizes spectral overlap, resulting in efficient energy transfer from the S_1/ICT state even for carotenoids having $N \sim 11$. This arrangement is crucial for AAPs because they live in the presence of oxygen, and therefore effective quenching of BChl-*a* triplet states and singlet oxygen is critical for the survival of these organisms. It is a well-known fact that carotenoids with $N \sim 11$ are optimized for singlet oxygen quenching[78] and also appear to be the most effective in quenching the triplet state of BChl-*a*.[79] These facts solidify the relationships between carotenoid conformation, activation of the ICT state, photoprotection, and light harvesting, thus demonstrating that the strategy reported previously for *Rba. sphaeroides* is widespread among phototrophic bacteria that encounter both light and oxygen.

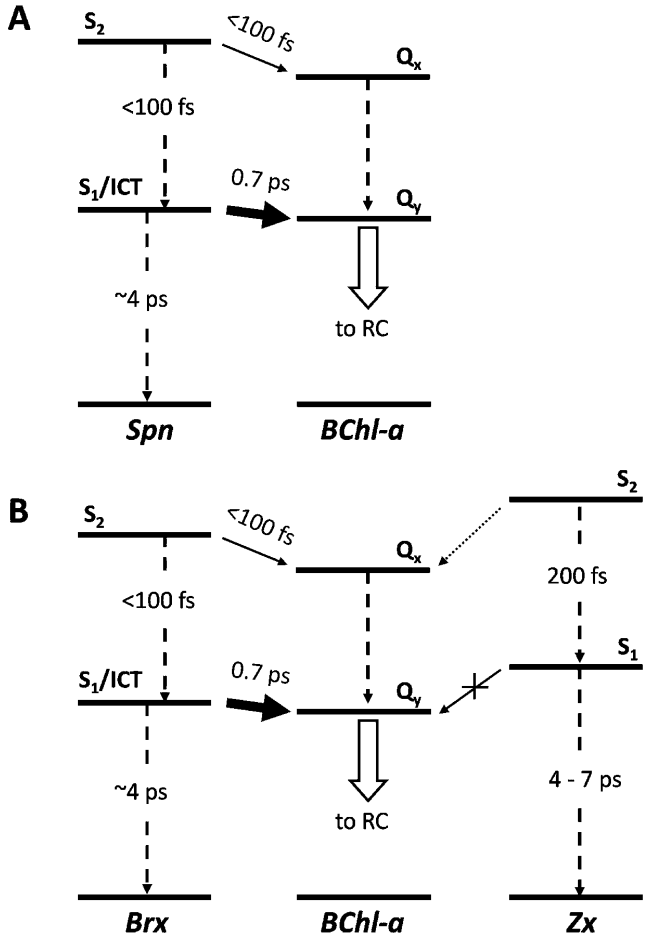

Figure 10. Scheme of energy transfer pathways for LH1−RC complexes of (A) *Roseobacter* sp. COL2P and (B) *Erythrobacter* sp. NAP1. Solid lines represent energy transfer channels, and the dotted line from the S_2 state of zeaxanthin denotes a possible minor energy transfer channel. Dashed lines represent internal conversion processes. Spn = spheroidenone, Brx = bacteriorubixanthinal, Zx = zeaxanthin.

ASSOCIATED CONTENT

Supporting Information

Chromatogram demonstrating purity of bacteriorubixanthinal, global fitting results of bacteriorubixanthinal in solution and of LH1−RC from *Roseobacter* sp. COL2P in carotenoid radical region, kinetics of carotenoid signals in the LH1−RC complexes vs in solution together with BChl-*a* bleaching signal, comparison of LH1−RC transient absorption spectra of *Roseobacter* sp. COL2P and *Rba. sphaeroides*, and transient absorption spectra of LH1−RC complexes from *Roseobacter* sp. COL2P and *Erythrobacter* sp. NAP1 after excitation at 866 nm. This material is available free of charge via the Internet at http://pubs.acs.org.

AUTHOR INFORMATION

Corresponding Author

*E-mail: tpolivka@jcu.cz.

Notes

The authors declare no competing financial interest.

ACKNOWLEDGMENTS

We thank Petr Hříbek, Pavel Chábera, and Miriam Enriquez for their help with femtosecond experiments. Jan Česal and Pavel Hrouzek are gratefully acknowledged for help with extraction of bacteriorubixanthinal and Dzmitry Hauruseu for growing the *Erythrobacter* and *Roseobacter* cultures. This work was supported by the Czech Science Foundation (P205/11/1164 and P501/12/G055), Grant Agency of the Academy of Sciences of the Czech Republic (IAA608170901), Grant Agency of University of South Bohemia (027/2011/P), and projects ME09037, MSM6007665808, AV0ZS0510513 and Algatech (CZ.1.05/2.1.00/03.0110) from the Ministry of Education of the Czech Republic. Work in the laboratory of HAF was supported by a grant from the National Science Foundation (MCB-0913022) and by the University of Connecticut Research Foundation.

REFERENCES

(1) Blankenship, R. E. *Molecular Mechanisms of Photosynthesis*; Blackwell Science: Oxford, U. K., 2002.

(2) Scholes, G. D.; Fleming, G. R.; Olaya-Castro, A.; van Grondelle, R. *Nature Chem.* **2011**, *3*, 764−774.

(3) Tronrud, D. E.; Wen, J.; Gay, L.; Blankenship, R. E. *Photosynth. Res.* **2009**, *100*, 79−87.

(4) Vulto, S. I. E.; Neerken, S.; Louwe, R. J. W.; de Baat, M. A.; Amesz, J.; Aartsma, T. J. *J. Phys. Chem. B* **1998**, *102*, 10630−10635.

(5) Brixner, T.; Stenger, J.; Vaswani, H. M.; Cho, M.; Blankenship, R. E.; Fleming, G. R. *Nature* **2005**, *434*, 625−628.

(6) Adolphs, J.; Renger, T. *Biophys. J.* **2006**, *91*, 2778−2797.

(7) McDermott, G.; Prince, S. M.; Freer, A. A.; Hawthornwaite-Lawless, A. M.; Papiz, M. Z.; Cogdell, R. J.; Isaacs, N. W. *Nature* **1995**, *374*, 517−521.

(8) Koepke, J.; Hu, X.; Muenke, C.; Schulten, K.; Michel, H. *Structure* **1996**, *4*, 581.

(9) Krueger, B. P.; Scholes, G. D.; Jimenez, R.; Fleming, G. R. *J. Phys. Chem. B* **1998**, *102*, 2284−2292.

(10) Macpherson, A. N.; Arellano, J. B.; Fraser, N. J.; Cogdell, R. J.; Gillbro, T. *Biophys. J.* **2001**, *80*, 923−930.

(11) Zhang, J.-P.; Fujii, R.; Qian, P.; Inaba, T.; Mizoguchi, T.; Koyama, Y.; Onaka, K.; Watanabe, Y. *J. Phys. Chem. B* **2000**, *104*, 3683−3691.

(12) Liu, Z. F.; Yan, H. C.; Wang, K. B.; Kuang, T. Y.; Zhang, J. P.; Gui, L. L.; An, X. M.; Chang, W. R. *Nature* **2004**, *428*, 287−292.

(13) Gradinaru, C. C.; van Stokkum, I. H. M.; Pascal, A. A.; van Grondelle, R.; van Amerongen, H. *J. Phys. Chem. B* **2000**, *104*, 9330−9342.

(14) Akimoto, S.; Yokono, M.; Ohmae, M.; Yamazaki, I.; Tanaka, A.; Higuchi, M.; Tsuchiya, T.; Miyashita, H.; Mimuro, M. *J. Phys. Chem. B* **2005**, *109*, 12612−12619.

(15) Croce, R.; Müller, M. G.; Bassi, R.; Holzwarth, A. R. *Biophys. J.* **2001**, *80*, 901−915.

(16) Walla, P. J.; Linden, P. A.; Ohta, K.; Fleming, G. R. *J. Phys. Chem. A* **2002**, *106*, 1909−1916.

(17) Hofmann, E.; Wrench, P. M.; Sharples, F. P.; Hiller, R. G.; Welte, W.; Diederichs, K. *Science* **1996**, *272*, 1788−1791.

(18) Polívka, T.; Hiller, R. G.; Frank, H. A. *Arch. Biochem. Biophys.* **2007**, *458*, 111−120.

(19) Bautista, J. A.; Hiller, R. G.; Sharples, F. P.; Gosztola, D.; Wasielewski, M.; Frank, H. A. *J. Phys. Chem. A* **1999**, *103*, 2267−2273.

(20) Zigmantas, D.; Hiller, R. G.; Sundström, V.; Polívka, T. *Proc. Natl. Acad. Sci. U.S.A.* **2002**, *99*, 16760−16765.

(21) Krueger, B. P.; Lampoura, S. S.; van Stokkum, I. H. M.; Papagiannakis, E.; Salverda, J. M.; Gradinaru, C. C.; Rutkauskas, D.; Hiller, R. G.; van Grondelle, R. *Biophys. J.* **2001**, *80*, 2843−2855.

(22) Polívka, T.; Sundström, V. *Chem. Rev.* **2004**, *104*, 2021−2071.

(23) Polívka, T.; Frank, H. A. *Acc. Chem. Res.* **2010**, *43*, 1125−1134.

(24) Koyama, Y.; Rondonuwu, F. S.; Fujii, R.; Watanabe, Y. *Biopolymers* **2004**, *74*, 2−18.

(25) Gradinaru, C. C.; Kennis, J. T. M.; Papagiannakis, E.; van Stokkum, I. H. M.; Cogdell, R. J.; Fleming, G. R.; Niederman, R. A.; van Grondelle, R. *Proc. Natl. Acad. Sci. U.S.A.* **2001**, *98*, 2364−2369.

(26) Polívka, T.; Sundström, V. *Chem. Phys. Lett.* **2009**, *477*, 1−11.

(27) Kleinschmidt, M.; Marian, C. M.; Waletzke, M.; Grimme, S. *J. Chem. Phys.* **2009**, *130*, 044708.

(28) Starcke, J. H.; Wormit, M.; Dreuw, A. *J. Chem. Phys.* **2009**, *130*, 024104.

(29) Frank, H. A.; Bautista, J. A.; Josue, J.; Pendon, Z.; Hiller, R. G.; Sharples, F. P.; Gosztola, D.; Wasielewski, M. R. *J. Phys. Chem. B* **2000**, *104*, 4569−4577.

(30) Zigmantas, D.; Hiller, R. G.; Sharples, F. P.; Frank, H. A.; Sundström, V.; Polívka, T. *Phys. Chem. Chem. Phys.* **2004**, *6*, 3009−3016.

(31) Roszak, A. W.; Howard, T. D.; Southall, J.; Gardiner, A. T.; Law, C. J.; Isaacs, N. W.; Cogdell, R. J. *Science* **2003**, *302*, 1969−1972.

(32) Šlouf, V.; Chábera, P.; Olsen, J. D.; Martin, E. C.; Qian, P.; Hunter, C. N.; Polívka, T. *Proc. Natl. Acad. Sci. U.S.A.* **2012**, *109*, 8570−8575.

(33) Akahane, J.; Rondonuwu, F. S.; Fiedor, L.; Watanabe, Y.; Koyama, Y. *Chem. Phys. Lett.* **2004**, *393*, 184−191.

(34) Papagiannakis, E.; van Stokkum, I. H. M.; Fey, H.; Büchel, C.; van Grondelle, R. *Photosynth. Res.* **2005**, *86*, 241−250.

(35) Polívka, T.; van Stokkum, I. H. M.; Zigmantas, D.; van Grondelle, R.; Sundström, V.; Hiller, R. G. *Biochemistry* **2006**, *45*, 8516−8526.

(36) Montano, G. A.; Xin, Y. Y.; Lin, S.; Blankenship, R. E. *J. Phys. Chem. B* **2004**, *108*, 10607−10611.

(37) Niedzwiedzki, D. M.; Collins, A. M.; LaFountain, A. M.; Enriquez, M. M.; Frank, H. A.; Blankenship, R. E. *J. Phys. Chem. B* **2010**, *114*, 8723−8734.

(38) Nakamura, R.; Nakagawa, K.; Nango, M.; Hashimoto, H.; Yoshizawa, M. *J. Phys. Chem. B* **2011**, *115*, 3233−3239.

(39) Yurkov, V. V.; Csotonyi, J. T. New light on aerobic anoxygenic phototrophs. In *The purple phototrophic bacteria*; Hunter, C. N., Daldal, F., Thurnauer, M. C., Beaty, J. T., Eds.; Springer Verlag: New York, U.S.A., 2009; pp 31−55.

(40) Yutin, N.; Suzuki, M. T.; Teeling, H.; Weber, M.; Venter, J. C.; Rusch, D. B.; Béjà, O. *Environ. Microbiol.* **2007**, *9*, 1464−1475.

(41) Kolber, Z. S.; Plumley, F. G.; Lang, A. S.; Beatty, J. T.; Blankenship, R. E.; VanDover, C. L.; Vetriani, C.; Koblizek, M.; Rathgeber, C.; Falkowski, P. G. *Science* **2001**, *292*, 2492−2495.

(42) Jiao, N.; Zhang, Y.; Zeng, Y.; Hong, N.; Liu, R.; Chen, F.; Wang, P. *Environ. Microbiol.* **2007**, *9*, 3091−3099.

(43) Koblížek, M. Role of photoheterotrophic bacteria in the marine carbon cycle. In *Microbial carbon pump in the ocean*; Jiao, N., Azam, F., Sanders, S., Eds.; Science/AAAS: Washington D. C., U.S.A., 2011.

(44) Koblížek, M.; Béjà, O.; Bidigare, R. R.; Christensen, S.; Benetiz-Nelson, B.; Vetriani, C.; Kolber, M. K.; Falkowski, P. G.; Kolber, Z. S. *Arch. Microbiol.* **2003**, *180*, 327−338.

(45) Koblížek, M.; Mlčoušková, J.; Kolber, Z.; Kopecký, J. *Arch. Microbiol.* **2010**, *192*, 41−49.

(46) Zigmantas, D.; Polívka, T.; Hiller, R. G.; Yartsev, A.; Sundström, V. *J. Phys. Chem. A* **2001**, *105*, 10296−10306.

(47) Shima, S.; Ilagan, R. P.; Gillespie, N.; Sommer, B. J.; Hiller, R. G.; Sharples, F. P.; Frank, H. A.; Birge, R. R. *J. Phys. Chem. A* **2003**, *107*, 8052−8066.

(48) Papagiannakis, E.; Larsen, D. S.; van Stokkum, I. H. M.; Vengris, M.; Hiller, R. G.; van Grondelle, R. *Biochemistry* **2004**, *43*, 15303−15309.

(49) Vaswani, H. M.; Hsu, C. P.; Head-Gordon, M.; Fleming, G. R. *J. Phys. Chem. B* **2003**, *107*, 7940−7946.
(50) Niedzwiedzki, D. M.; Fuciman, M.; Frank, H. A.; Blankenship, R. E. *Biochim. Biophys. Acta* **2011**, *1807*, 518−528.
(51) Cong, H.; Niedzwiedzki, D. M.; Gibson, G. N.; LaFountain, A. M.; Kelsh, R. M.; Gardiner, A. T.; Cogdell, R. J.; Frank, H. A. *J. Phys. Chem. B* **2008**, *112*, 10689−10703.
(52) van Stokkum, I. H. M.; Larsen, D. S.; van Grondelle R., D. S. *Biochim. Biophys. Acta* **2004**, *1657*, 82−104.
(53) Cogdell, R. J.; Howard, T. D.; Isaacs, N. W.; McLuskey, K.; Gardiner, A. T. *Photosynth. Res.* **2002**, *74*, 135−141.
(54) Pan, J.; Lin, S.; Allen, J. P.; Williams, J. C.; Frank, H. A.; Woodbury, N. W. *J. Phys. Chem. B* **2011**, *115*, 7058−7068.
(55) Frank, H. A.; Cua, A.; Chynwat, V.; Young, A.; Gosztola, D.; Wasielewski, M. R. *Photosynth. Res.* **1994**, *41*, 389−395.
(56) Billsten, H. H.; Zigmantas, D.; Sundström, V.; Polívka, T. *Chem. Phys. Lett.* **2002**, *355*, 465−470.
(57) Polívka, T.; Herek, J. L.; Zigmantas, D.; Åkerlund, H.-E.; Sundström, V. *Proc. Natl. Acad. Sci. U.S.A.* **1999**, *96*, 4914−4917.
(58) Chábera, P.; Fuciman, M.; Hříbek, P.; Polívka, T. *Phys. Chem. Chem. Phys.* **2009**, *11*, 8795−8803.
(59) Polívka, T.; Kerfeld, C. A.; Pascher, T.; Sundström, V. *Biochemistry* **2005**, *44*, 3994−4003.
(60) Wilson, A.; Punginelli, C.; Gall, A.; Bonetti, C.; Alexandre, M.; Routaboul, J. M.; Kerfeld, C. A.; van Grondelle, R.; Robert, B.; Kennis, J. T. M.; et al. *Proc. Natl. Acad. Sci. U.S.A.* **2008**, *105*, 12075−12080.
(61) Billsten, H. H.; Pan, J. X.; Sinha, S.; Pascher, T.; Sundström, V.; Polívka, T. *J. Phys. Chem. A* **2005**, *109*, 6852−6859.
(62) Polívka, T.; Pullerits, T.; Frank, H. A.; Cogdell, R. J.; Sundström, V. *J. Phys. Chem. B* **2004**, *108*, 15398−15407.
(63) Polívka, T.; Niedzwiedzki, D.; Fuciman, M.; Sundström, V.; Frank, H. A. *J. Phys. Chem. B* **2007**, *111*, 7422−7431.
(64) Jeevarajan, J. A.; Wei, C. C.; Jeevarajan, A. S.; Kispert, L. D. *J. Phys. Chem.* **1996**, *100*, 5637−5641.
(65) Niedzwiedzki, D. M.; Chatterjee, N; Enriquez, M. M.; Kajikawa, T.; Hasegawa, S.; Katsumura, S.; Frank, H. A. *J. Phys. Chem. B* **2009**, *113*, 13604−13612.
(66) Enriquez, M. M.; Fuciman, M.; LaFountain, A. M.; Wagner, N. L.; Birge, R. R.; Frank, H. A. *J. Phys. Chem. B* **2010**, *114*, 12416−12426.
(67) Kerfeld, C. A.; Sawaya, M. R.; Brahmandam, V.; Cascio, D.; Ho, K. K.; Trevithick-Sutton, C. C.; Krogmann, D. W.; Yeates, T. O. *Structure* **2003**, *11*, 55−65.
(68) Zigmantas, D.; Hiller, R. G.; Yartsev, A.; Sundström, V.; Polívka, T. *J. Phys. Chem. B* **2003**, *107*, 5339−5348.
(69) Kosumi, D.; Kusumoto, T.; Fujii, R.; Sugisaki, M.; Iinuma, Y.; Oka, N.; Takaesu, Y.; Taira, T.; Iha, M.; Frank, H. A.; et al. *Phys. Chem. Chem. Phys.* **2011**, *13*, 10762−10770.
(70) Wohlleben, W.; Buckup, T.; Herek, J. L.; Cogdell, R. J.; Motzkus, M. *Biophys. J.* **2003**, *85*, 442−450.
(71) Fujii, R.; Inaba, T.; Watanabe, Y.; Koyama, Y.; Zhang, J. P. *Chem. Phys. Lett.* **2003**, *369*, 165−172.
(72) Niedzwiedzki, D.; Koscielecki, J. F.; Cong, H.; Sullivan, J. O.; Gibson, G. N.; Birge, R. R.; Frank, H. A. *J. Phys. Chem. B* **2007**, *111*, 5984−5998.
(73) Picorel, R.; Bélanger, G.; Gingras, G. *Biochemistry* **1983**, *22*, 2491−2497.
(74) Broglie, R. M.; Hunter, C. N.; Delepelaire, P.; Niederman, R. A.; Chua, N.-H.; Clayton, R. K. *Proc. Natl. Acad. Sci. U.S.A.* **1980**, *77*, 87−91.
(75) Karrasch, S.; Bullough, P. A.; Ghosh, R. *EMBO J.* **1995**, *14*, 631−638.
(76) Jungas, C.; Ranck, J.; Rigaud, J.; Joliot, P.; Vermeglio, A. *EMBO J.* **1999**, *18*, 534−542.
(77) Qian, P.; Hunter, C. N.; Bullough, P. A. *J. Biol. Chem.* **2005**, *349*, 948−960.
(78) Di Mascio, P.; Kaiser, S.; Sies, H. *Arch. Biochem. Biophys.* **1989**, *274*, 532−538.
(79) Kakitani, Y.; Akahane, J.; Ishii, H.; Sogabe, H.; Nagae, H.; Koyama, Y. *Biochemistry* **2007**, *46*, 2181−2197.